1998

Analysis of Cell Division and Elongation Underlying the Developmental Acceleration of Root Growth in Arabidopsis Thaliana

Tobias Baskin, *University of Massachusetts - Amherst*
G.T.S. Beemster

Plant Physiol. (1998) 116: 1515–1526

Analysis of Cell Division and Elongation Underlying the Developmental Acceleration of Root Growth in *Arabidopsis thaliana*[1]

Gerrit T.S. Beemster and Tobias I. Baskin*

Division of Biological Sciences, University of Missouri, Columbia, Missouri 65211–7400

To investigate the relation between cell division and expansion in the regulation of organ growth rate, we used *Arabidopsis thaliana* primary roots grown vertically at 20°C with an elongation rate that increased steadily during the first 14 d after germination. We measured spatial profiles of longitudinal velocity and cell length and calculated parameters of cell expansion and division, including rates of local cell production (cells mm^{-1} h^{-1}) and cell division (cells $cell^{-1}$ h^{-1}). Data were obtained for the root cortex and also for the two types of epidermal cell, trichoblasts and atrichoblasts. Accelerating root elongation was caused by an increasingly longer growth zone, while maximal strain rates remained unchanged. The enlargement of the growth zone and, hence, the accelerating root elongation rate, were accompanied by a nearly proportionally increased cell production. This increased production was caused by increasingly numerous dividing cells, whereas their rates of division remained approximately constant. Additionally, the spatial profile of cell division rate was essentially constant. The meristem was longer than generally assumed, extending well into the region where cells elongated rapidly. In the two epidermal cell types, meristem length and cell division rate were both very similar to that of cortical cells, and differences in cell length between the two epidermal cell types originated at the apex of the meristem. These results highlight the importance of controlling the number of dividing cells, both to generate tissues with different cell lengths and to regulate the rate of organ enlargement.

A central question in plant physiology is how plants regulate their growth rate. The growth rate of a plant organ changes with development and as the plant responds to stimuli. Growth rate is regulated by the combined activity of two linked processes, expansion and cell production. Although organ growth rate is determined by expansion directly, growth rate is also influenced by cell production, through the determination of how many cells are expanding at a given time. Conversely, expansion may partially regulate cell production, because it displaces cells from the meristem and because it is required for continued cell division. Studies of the regulation of growth rate have rarely measured expansion in the meristem, and studies that measure cell division rates have rarely quantified expansion concurrently. To understand how plants regulate the growth of their organs, we need to quantify expansion throughout the growth zone as well as cell production.

The rate of cell production by a meristem has two distinct components: the number of dividing cells and their rate of division. The number of dividing cells is determined by their size and by the size of the meristem, whereas the rate of cell division is determined by the regulation of the cell cycle. Therefore, an equivalent change in cell production could be caused by distinct mechanisms. Increases in the number of dividing cells could be caused by prolonging the expression of cell cycle machinery, whereas increases in the rate of division could be caused by enhancing the passage through cell cycle checkpoints. It is not known to what extent plants regulate cell production by either type of mechanism.

We have addressed the relationship between cell production and expansion in the root of *Arabidopsis thaliana*. We used a kinematic method that allows production and expansion rates to be quantified under identical conditions, even on the same roots, and quantifies the number of dividing cells as well as rates of cell division. A kinematic approach is ideally applied to *A. thaliana* roots because their diameter is constant over the growth zone, except for the very apical region, and cortical and epidermal cells occur in only a single tier each (Dolan et al., 1993). Moreover, cell length can be measured in living roots by using Nomarski microscopy, thereby avoiding fixation, embedding, sectioning, and the attendant shrinkage (Baskin et al., 1995).

Kinematic methods were pioneered decades ago (Goodwin and Stepka, 1945; Erickson and Sax, 1956; Hejnowicz, 1956), but although these methods have been used often to measure rates of expansion, they have seldom been used for measurements of division. Instead, investigators have relied on other methods for quantifying cell division rates, including mitotic index, rate of accumulation of metaphase cells after colchicine application, and the fraction of labeled mitoses after application of a pulse of tritiated thymidine. All of these methods were developed for homogeneous cell cultures. In organs, they have serious pitfalls and have produced contradictory results (Green and Bauer, 1977; Webster and Macleod, 1980). By contrast, these pitfalls are avoided by kinematic methods (Sacks et al., 1997). For

[1] This work was supported by a postdoctoral fellowship to G.T.S.B. from the University of Missouri Molecular Biology Program, by the Cooperative States Research Service, U.S. Department of Agriculture under agreement no. 92-37304-7868 (with T.I.B.), and by grant no. 94ER20146 to T.I.B. from the U.S. Department of Energy, which does not constitute endorsement by that department of views expressed herein.

* Corresponding author; e-mail baskin@biosci.mbp.missouri.edu; fax 1–573–882–0123.

quantifying cell production, the kinematic approach was set on a stronger mathematical foundation by the introduction of the continuity equation (Silk and Erickson, 1979; Gandar, 1980; Silk, 1984), which allows the production of cells to be treated analogously to the production of any substance, such as sucrose. Only in the last few years has there been a renewed use of kinematics for quantifying cell division rates (Ben-Haj-Salah and Tardieu, 1995; Beemster et al., 1996; Sacks et al., 1997).

The primary root of *A. thaliana*, like that of many other species, grows more rapidly with time from germination (Baskin et al., 1995). This acceleration happens naturally (without exogenous hormones) and is large, with rates doubling over several days. Therefore, we have chosen this system to investigate how growing organs coordinate cell production and expansion. In an earlier study of accelerating growth in the *A. thaliana* root, the increasing growth rate was found to be accompanied by increased cell production, which was argued to explain the enhanced elongation (Baskin et al., 1995). However, that study measured expansion indirectly and did not measure rates of cell division. For the increasing growth rate of the root, the aim of the present study was to resolve the contributions from expansion and cell production. Our results show that accelerating root elongation rates are accompanied by increased cell production in the meristem, with little change in cellular expansion rates. These results suggest that the number of growing cells regulates root growth rate directly.

MATERIALS AND METHODS

Seeds of *Arabidopsis thaliana* L. (Heynh), ecotype Columbia, were stored at 4°C. At d 0, they were surface sterilized with 15% household bleach and plated on agar-solidified, modified Hoagland solution in 90 × 90 mm^2 square tissue culture plates, which were then placed vertically in a growth chamber under constant conditions (20°C, 80 μmol of light m^{-2} s^{-1}; Baskin and Wilson, 1997).

Velocity and Longitudinal Strain Rates

On d 6, 8, and 10, three roots on each of five different plates were selected for similar length and growth rate (estimated by eye from marks on the bottom of the plate indicating the position of the root tip on previous days). Under a dissecting microscope, graphite particles (Mr. Zip, extra fine, A.G.S. Co., Muskegon, MI) were sprinkled on the upper surface of roots with an eyelash mounted on an applicator. After 1 h, the root with the least tendency to rotate was selected from the marked roots on each plate and was used for subsequent observations of particle positions. A plate was removed from the growth chamber and placed vertically on a horizontally oriented compound microscope fitted with a ×10 objective and a charge-coupled device camera (C2400, Hamamatsu Co., Hamamatsu, Japan). A series of overlapping images was recorded on videotape in S-VHS format with the time stamped on each image by a time-date generator and the plate was returned to the growth chamber. On a given day, five roots were followed, and five or six observations were made of each root at intervals of about 1 h. Subsequently, images from the videotape were captured with an Apple Macintosh 7100/66 computer equipped with a frame grabber board (LG3, Scion Corp., Frederick, MD), and composite images of individual roots were created for each observation time. All image processing and analyses were done with the public domain NIH Image program (version 1.60; National Institutes of Health; available at http://rsb.info.nih.gov/nih-image/).

The position of individual particles relative to the tip of the root was measured in each pair of images. Velocities of displacement ($v[x]$; μm h^{-1}) were then calculated as:

$$v(x) = \frac{x_{i,2} - x_{i,1}}{t_2 - t_1} \quad (1)$$

where $x_{i,t}$ is the ith particle at time t, and $x = 0.5 * (x_{i,1} + x_{i,2})$. Subsequently, values of x were adjusted to represent distance from the quiescent center by subtracting the length of the root cap (see below). For observations made on a given day, we were unable to detect a significant change in the velocity profile over the observation interval (5–6 h). Therefore, the resulting four to five velocity data sets obtained for each root were combined and then smoothed and interpolated into 25-μm spaced points.

The smoothing procedure fitted a series of overlapping, independent polynomials to the data. First, a given number of data points was selected symmetrically around the first desired x and the parameters of a third-degree polynomial fitted to this interval were used to calculate $v(x)$. The value of x was then increased by 25 μm and the process was repeated. For positions at the beginning and end of the series, the data were not symmetric around x but contained the same number of points. The data thus obtained were not smooth enough to permit meaningful differentiation required for subsequent calculations. Therefore, a second step was introduced, in which the equally spaced data obtained from step 1 were smoothed further using a similar procedure. This second step was repeated until the change in velocity between successive iterations became smaller than 1 μm h^{-1} for all points of the data set. To adjust for differences in numbers of observations between individual roots, the number of data points for step 1 was defined as the number of points between the tip of the root and the location where velocity started to increase rapidly (Fig. 2, inset; between 50 and 120 points), and the length of this root segment defined the interval for step 2 (250–450 μm). The smoothing procedure was relatively insensitive to the interval's length. The smoothing algorithm was implemented as a macro for the program ProFit (version 5.0, QuantumSoft, Zürich, Switzerland).

From the smoothed data, the length of the growth zone was determined as the distance between the quiescent center and the first position where the increase in velocity between successive positions was less than or equal to 0. Final velocity, which equals the rate at which the root elongated, was found by averaging the velocity over all points basal to the end of the growth zone. We used the final round of fitted polynomials to calculate strain rates

($r[x]$; % h^{-1}), the derivative of velocity with respect to distance along the root:

$$r(x) = 100 \times \frac{\delta v}{\delta x} \quad (2)$$

Analysis of Cell Length

Directly after video recording, the plates were stored at 4°C to minimize further growth. Individual roots were mounted in the nutrient solution within chambers, which prevented deformation of the root and which could be flipped over to allow cells in both halves of the root to be observed. The roots were viewed under Nomarski optics (Zeiss Axioplan) with a ×40, 0.9-numerical aperature objective. A series of overlapping images of cortical and epidermal cell files from several focal planes were captured using a charge-coupled device camera (VI-470; Optronics Engineering, Goleta, CA) fitted to the microscope and connected to a 486 PC running Image1/AT software (Universal Imaging, West Chester, PA). The series of images continued until cell length exceeded the width of the video image (when average cell size was approximately 100 μm). Composite images were created and used to measure the length of every cell in each cortical and epidermal cell file that could be followed over most of its length. The position of each cell was defined by its midpoint. The length of the root cap was determined separately on images through the median plane, as the distance between the tip of the root and the basal margin of the quiescent center.

Cell lengths from all files of a given cell type were combined for each root and then smoothed and interpolated with the same procedure as used for the velocity data. The number of data points used to define the interval for step 1 was determined as the number of cells between the inflection point where cell length started to increase (Fig. 3) and the most basal data point and ranged from 15 to 40. The length of the interval used for step 2 was defined as the distance between the same inflection point and the quiescent center and ranged between 250 and 550 μm. The iteration in step 2 was repeated until the change in cell length between successive iterations became smaller than 0.5 μm for all positions.

Analysis of Cell Division

Cell flux ($F[x]$; cells h^{-1}), the rate at which cells flow past a particular position x, was calculated from:

$$F(x) = \frac{v(x)}{l(x)} \quad (3)$$

The increase in $F(x)$ is proportional to local rates of cell production. This relationship is explicit in the continuity equation (Silk and Erickson, 1979; Gandar, 1980; Silk, 1984), which we used to calculate local cell production rates ($P[x]$; cells μm^{-1} h^{-1}):

$$P(x) = \frac{\delta F}{\delta x} + \frac{\delta \rho(x)}{\delta t} \quad (4)$$

where $\rho(x)$ is cell density, the inverse of cell length. The term $\delta F/\delta x$ was calculated directly from the cell flux profile of each root, using five-point, second-degree differentiation formulas (Erickson, 1976). The term $\delta\rho(x)/\delta t$, which equals 0 for all x under steady-state conditions, cannot be calculated for individual roots, since cell length for each root was observed only once. Therefore, this term was calculated for each of the three observation days from densities averaged over all roots, using three-point, second-degree differentiation formulas (Erickson, 1976).

Cell division rates ($D[x]$; cell $cell^{-1}$ h^{-1}) were calculated from $P(x)$ by correcting for cell length using:

$$D(x) = P(x) \times l(x) \quad (5)$$

In contrast to terminology used recently by Sacks et al. (1997), we call P, the direct result of the continuity equation, a "cell production rate." By doing so, we adhere to the terminology proposed earlier by Gandar (1980) and avoid confusing this parameter with a "cell division rate." The rate of cell division is widely understood as being on a per cell basis and inversely proportional to cell cycle duration.

The position of the end of the division zone was determined for individual roots as the location where $P(x)$ first became 0 or negative. In a few roots, $P(x)$ stabilized at small but positive values, and the end of the division zone of these roots was taken as the position where $P(x)$ became approximately constant. The cell flux at this position was defined as "final cell flux" (F_f) and represents the total rate of cell production for each file.

The cumulative number of cells per file, $n(x)$, was calculated from cell density data using:

$$n(x) = 25 \times \sum_{25}^{x} \frac{(\rho[x] + \rho[x - 25])}{2} \quad (6)$$

with $x = 25, 50, 75. \ldots$. The profile of n was then used to determine cell numbers for defined regions of the root.

Average cell division rate for the whole of the meristem ($\overline{D}$; h^{-1}) was calculated for each root from the final cell flux and the number of dividing cells (N_{div}):

$$\overline{D} = \frac{F_f}{N_{div}} \quad (7)$$

Given the exponential nature of the cell division process, the average cell cycle duration ($\overline{T}_c$; h) can be calculated from N_{div} and F_f (Green, 1976; Webster and Macleod, 1980; Ivanov, 1994) as:

$$\overline{T}_c = \ln(2) \times \frac{N_{div}}{F_f} \quad (8)$$

Temporal (Lagrangian) Quantification

Because root growth is not steady in *A. thaliana* seedling roots (see "Results"), we cannot easily transform the spatial (Eulerian) data into temporal (Lagrangian) data expressing the development of a material element as it moves through the growth zone (Silk, 1984). However, the time it takes for a cell to move through the elongation zone (T_{el}) is relatively

short, so the number of cells in the elongation zone (N_{el}) and the flux of cells through that zone (F_f) do not change much during this period. Therefore, T_{el} can be estimated from:

$$T_{el} = \frac{N_{el}}{F_f} \quad (9)$$

A true residence time for individual cells in the meristem cannot be calculated because each cell exists only from its formation until it undergoes cytokinesis. For the majority of cells, residence time would therefore equal cell cycle duration. However, if the average cell cycle duration in the meristem is approximately constant over time, we can calculate residence time of the most basal transverse wall in the file by assuming it was formed by a division of the most apical cell in the file. Accordingly, residence time in the meristem (T_{div}; h) is directly proportional to the number of division cycles it takes to form all cells in the meristem and was calculated as:

$$T_{div} = \overline{T}_c \times \log_2(N_{div}) \quad (10)$$

Tests of the Curve-Fitting Procedure

Various methods have been used to smooth and interpolate cell length and velocity data. One approach is to fit a logistic function to the data (Barlow et al., 1991; Morris and Silk, 1992). Although these functions fit this type of data approximately, there is no reason to expect an exact fit, and they may deviate systematically from the true distribution. Therefore, a nonparametric smoothing method is preferable. A method commonly used for this type of problem is cubic (β) splines. To test curve-fitting procedures, we used a function to generate simulated data sets and compared the real solution, obtained analytically from the function, to the approximation from curve fitting. The function used was a modified logistic function (Morris and Silk, 1992) with parameters adjusted to resemble d 10 plants. Real data were simulated by adding random "noise" having the same variance as the original cell length or velocity data. Splines were fitted to the simulated data using procedure "TRANSREG" of the SAS statistical package (SAS Institute, Cary, NC), with one knot for the cell length and nine knots for the velocity data giving optimal results.

The splines and our method both seemed to fit velocity (not shown) and cell length data (Fig. 1A) well. However, when a derivative was examined (e.g. strain rate), the results from the spline fit deviated from the function's derivative more than the results of our method (Fig. 1B); when two simulated data sets were combined as required to calculate cell production rates, the results of the spline fit deviated notably from the analytical solution (Fig. 1C). We repeated this test twice on different simulated data sets with similar results.

Statistical Analysis

The experiment was repeated twice, for a total of 10 replicate plants per observation day. Statistical significance of differences between d 6, 8, and 10 for all parameters was determined by multivariate analysis of variance with Statistica (PC version 5.1, StatSoft, Inc., Tulsa, OK).

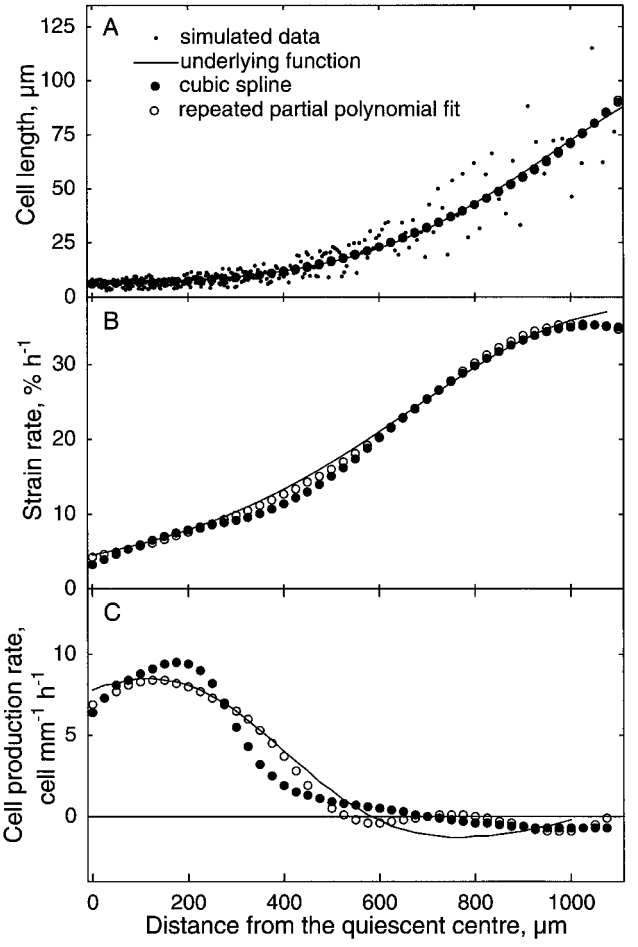

Figure 1. Comparison of curve fitting with cubic (β) splines and repeated partial polynomials. A modified logistic function (Morris and Silk, 1992) was fitted to the velocity and cell length data of a d 10 plant, and random noise, with variance equal to that of the actual data, was added to generate simulated data sets. Each data set was smoothed and interpolated using cubic splines or repeated partial polynomials, and strain rates and cell division parameters were calculated as described in "Materials and Methods." A, Cell length; B, strain rate; C, cell production rate. In B and C, the solid line plots the analytical solution of the function.

RESULTS

We analyzed cell division and expansion in the longitudinal direction only, simplifying the root as a single file for each cell type under study. This assumption is reasonable because in the *A. thaliana* root lateral expansion and formative divisions are restricted to the very apical part of the growth zone (Dolan et al., 1993). We measured velocity and cell length as a function of position along the root axis and used these data to calculate spatial profiles of expansion and cell division. Because velocity and cell length profiles were measured on the same root, all of the required calcu-

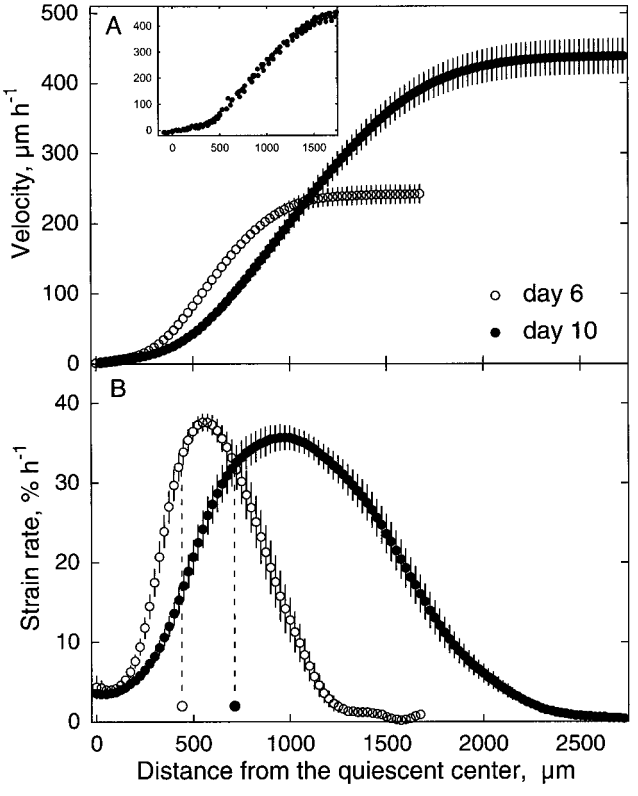

Figure 2. Spatial profiles of longitudinal velocity and strain rate of *A. thaliana* roots on d 6 and 10. Data from each root were smoothed and interpolated as described in "Materials and Methods"; symbols are means ± SE (when larger than the symbol) of 10 roots. A, Velocity; the inset shows raw data points for a single d 10 root. The final velocity on d 6 was 241 ± 6 μm h^{-1} and on d 10 it was 445 ± 12 μm h^{-1}. B, Strain rate; symbols on the *x* axis and the vertical dashed lines mark the basal terminus of the meristem averaged from individual roots.

lations were made on an individual root basis, which allowed us to estimate the variability between roots for all parameters.

Velocity and Strain Rate Profiles

Measurements of velocity as a function of position often showed a relatively sharp transition, from a shallow rate of increase near the apex to a steeper rate more basally (Fig. 2A, inset). This prominent transition was absent from the averages over 10 roots (Fig. 2A), because the transition occurred at different locations for individual roots. The final velocity (i.e. overall root elongation rate) on d 10 was nearly twice that of d 6, reflecting a 16.6% increase per day, similar to that reported by Baskin et al. (1995). These average final velocities were about 10% less than elongation rates of unmarked roots on the same plates, as determined by marks on the bottom of the plate at the position of the root tip on each day.

Increased root growth rates arose primarily from an increase in the longitudinal extent of the growth zone, whereas both the shape of the strain rate profile and maximal strain rates remained the same (Fig. 2B). Note that strain rates did not decrease to 0 at the apex; instead, in the apical few hundred micrometers, strain rates remained approximately constant, at about 4% h^{-1}. Between d 6 and 10, the average length of the growth zone, defined as the distance between the quiescent center and the position where strain rate first reached 0, nearly doubled (Table I). Thus, the increasing root velocity was caused by an enlarging growth zone, without increased maximal strain rate.

Cell Flux

In the apical region of the growth zone, the profile of cortical cell length was gently concave downward, which is typical of root tissues, and with time the extent of the region of small cells increased (Fig. 3A). The flux of cells at

Table I. *Spatial and temporal dimensions of the growth zone and its components for cortical cells in A. thaliana roots*

Data are the means ± SE of 10 roots. Delineation of growth zone and meristem length is described in "Materials and Methods," and the length of the zone of rapid elongation was defined as their difference. The number of cells within each zone, and their residence time, was calculated as described in "Materials and Methods." Significance denotes the overall significance of the difference between days, determined by multivariate analysis of variance.

Parameter	Zone	Day			Significance
		6	8	10	
Length (μm)	Growth	1231 ± 28	1850 ± 82	2337 ± 92	$P < 0.001$
	Meristem	440 ± 33	488 ± 42	713 ± 53	$P < 0.001$
	Rapid elongation	791 ± 39	1362 ± 92	1625 ± 66	$P < 0.001$
Cell no.	Growth	51 ± 2	68 ± 3	85 ± 3	$P < 0.001$
	Meristem	41 ± 2	52 ± 3	70 ± 3	$P < 0.001$
	Rapid elongation	10 ± 1	16 ± 2	15 ± 1	$P = 0.022$
Residence time (h)	Growth	99 ± 4	115 ± 9	127 ± 9	$P = 0.006$
	Meristem	93 ± 4	107 ± 9	121 ± 9	$P = 0.001$
	Rapid elongation	5.9 ± 0.9	7.7 ± 0.9	6.3 ± 0.5	NS[a]

[a] NS, Not significant.

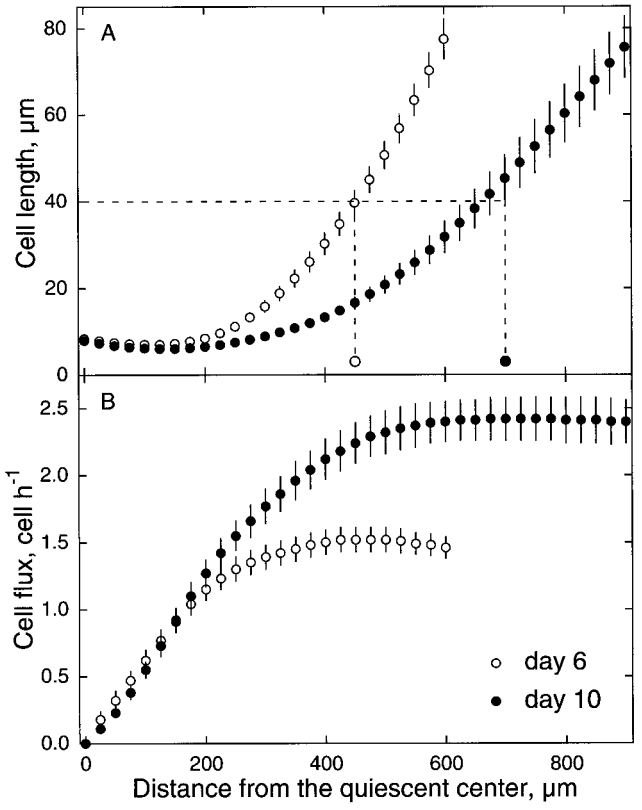

Figure 3. Spatial profiles of cell length and cell flux of cortical cells on d 6 and 10. Symbols are means ± SE (when larger than the symbol) of 10 roots. A, Cell length; symbols on the *x* axis and vertical dashed lines indicate the average length of the meristem for individual roots, and the horizontal dashed line indicates the cell length at the end of the meristem averaged over all roots. Data from each root were smoothed and interpolated as described in "Materials and Methods." B, Cell flux; the final cell flux was 1.68 ± 0.09 cells h^{-1} on d 6 and 2.55 ± 0.18 cells h^{-1} on d 10 (mean ± SE).

a given position, i.e. the number of cells passing that position per time, can be calculated by dividing that position's velocity by cell length (Eq. 3). Because velocity increased with distance from the quiescent center and cell length remained approximately constant, cell flux increased in the apical part of the growth zone until reaching a plateau (Fig. 3B). The maximal cell flux, which equals the total production rate of cells per file, increased significantly between d 6 and 10.

The increase in total cell production rate was slightly less than the increase in root elongation rate (1.6-fold for cell flux versus 1.8-fold for root elongation rate). This indicates that the extent of cellular elongation also increased, even though maximal strain rates did not increase (Fig. 2B). This increased elongation predicts that final cell length would have increased somewhat (by 1.2-fold), which is similar to the value previously found (Baskin et al., 1995). Therefore, during the developmental acceleration of root elongation rate, greater cell flux increased the number of elongating cells, but there was only a small change in the elongation of individual cells.

Cell Division

The increased rates of cell production by the meristem could be due to either increased size of the meristem or increased rates of cell production per unit length of the meristem. Local cell production rates in the meristem can be calculated from the local increase in the cell flux profile added to the local rate of change in cell density, as expressed by the continuity equation (Eq. 4; Silk and Erickson, 1979; Gandar, 1980; Silk, 1984). Except for the most apical 100 μm, cell production rates were higher on d 10 than on d 6 throughout the division zone (Fig. 4A). Both maximal cell production rate and the extent of the region of cell production increased. The average length of the meristem, determined for individual roots as the position where cell production rates first reached 0, increased by 62% from d 6 to 10 (Table I). As a consequence of the increasing length of both parts of the growth zone, the number of cells in the meristem and zone of rapid elongation steadily increased (Table I).

Cell production rates per unit length may be significant physiologically (Ben-Haj-Salah and Tardieu, 1995; Sacks et al., 1997); for example, these rates might reflect the abundance of a regulatory factor with an activity proportional to its concentration. However, cell division is naturally considered on a per cell basis, because a cell can be produced

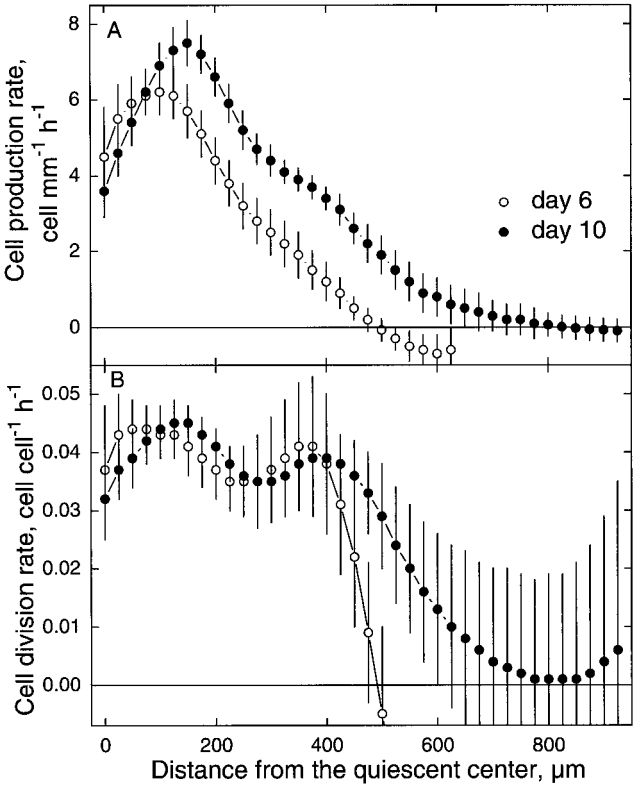

Figure 4. Spatial profiles of cell production rate and cell division rate in cortical cells on d 6 and 10. Cell production and division rates were calculated for each root as described in "Materials and Methods"; symbols are means ± SE (when larger than the symbol) of 10 roots.

only by another cell and not by an arbitrary length of meristem. A rate of cell division per cell can be calculated as an average for the entire meristem by dividing total cell flux by the number of cells in the meristem (Eq. 7). Also, local rates of cell division per cell can be calculated by correcting local cell production rates for differences in cell length (Eq. 5). The average rate of cell division was constant from d 6 through 10 (Table II). Consequently, the average cell cycle duration, calculated as the inverse of cell division rate and corrected for the exponential nature of the cell division process (Eq. 8), was also constant (Table II). The cell cycle averaged 18.6 ± 0.7 h (mean ± SE, $n = 30$), which is shorter than the 20 to 25 h previously reported for cortical cells in *A. thaliana* by other methods (Fujie et al., 1993; Baskin et al., 1995).

Although rates of cell production increased over time throughout most of the meristem (Fig. 4A), this was not reflected in parallel increases in cell division rates, which instead remained approximately constant throughout the meristem (Fig. 4B). For the basal part of the curve shown for d 10, the large SES resulted from large values of cell length in this region amplifying small deviations from 0 of the calculated local cell production rates, as well as from differences among roots in the location where cell production rates decreased rather abruptly to 0. Evidently, cell production was increased entirely by the increased number of dividing cells.

Surprisingly, when the extent of the division zone was compared with the spatial profile of expansion (Fig. 2B), cell division activity continued until strain rates almost reached their maximum. Similarly, cell division continued well beyond the location where cell length started to increase. The average size at which cells left the meristem was 39.5 ± 4.1 μm (mean ± SE, $n = 30$) and varied little with time, despite the fact that this length was reached at different distances from the quiescent center (Fig. 3A).

Temporal Analysis of Cell Expansion and Division

Thus far, we have focused on spatial aspects of cell expansion and division, quantifying these processes with respect to position along the root axis. However, the spatial distribution of cell expansion and division could be a reflection of the temporal regulation of these processes. For example, the size of the meristem could be regulated by the number of times a given cell is allowed to divide; similarly, the size of the elongation zone could be regulated by cells rapidly elongating for a set amount of time. It is therefore important to determine both spatial (Eulerian) and temporal (Lagrangian) aspects of cell division and expansion (Silk, 1984).

For the zone of rapid elongation, despite its enlargement over time (Fig. 2), residence time did not increase significantly (Table I), which along with the similar maximal strain rates indicates that the elongation behavior of a cell as it moved through the zone did not change. Actually, the extent of cellular elongation was expected to have increased because of the predicted increase in final cell length. If the increased cellular elongation were due to only increased residence time in the zone of rapid elongation, then the magnitude of the expected increase would be only 0.7 h, which is too small to have been detected (Table I) and could easily have been missed. For the meristem, we used Equation 10 to calculate residence time because average cell cycle duration was essentially constant over time. On successive days, a cell wall formed by division of the most apical cell took progressively longer to migrate through the meristem (Table I). In other words, as the meristem developed, cells continued dividing for longer periods. Prolonging cell division could be the regulatory event that increased the total rate of cell production and increased the growth rate of the root.

Cell Production and Cell Division in Epidermal Cells

Results thus far have concerned division and expansion only in cortical cells. For various species, tissues differ in the position of the basal terminus of cell division (Rost and Baum, 1988), and they may also differ in other parameters of cell division; however, to our knowledge this has been studied only with nonkinematic methods. In *A. thaliana*, the epidermis contains two cell types, which are segregated in files. Cells in one type of file nearly always make root hairs (trichoblasts) and cells in the other type rarely make hairs (atrichoblasts; Dolan, 1996). The atrichoblasts are longer than trichoblasts at maturity, which indicates that atrichoblast files produce fewer cells than do trichoblast files (because the two types of file must have the same longitudinal velocity at any given position). To determine the basis for the lowered cell production of atrichoblasts, as

Table II. *Average cell division rate and cell cycle duration of cortical cells*

Average cell division rate ($\overline{D}$) and cell cycle duration ($\overline{T}_c$) over the whole of the meristem at 6, 8, and 10 d after sowing (mean ± SE; $n = 10$). Average cell division rate was calculated as the total cell production in the meristem, i.e. final flux, divided by the number of cells in the meristem; the average cell cycle duration was calculated as the inverse of average division rate multiplied by ln(2) (see "Materials and Methods"). Significance denotes the overall significance of the difference between days, determined by multivariate analysis of variance.

Parameter	Day			Significance
	6	8	10	
$\overline{D}$ (cell cell^{-1} h^{-1})	0.041 ± 0.002	0.039 ± 0.003	0.037 ± 0.002	NS[a]
$\overline{T}_c$ (h)	17.3 ± 0.7	18.7 ± 1.5	19.8 ± 1.4	NS

[a] NS, Not significant.

well as to compare both types of cells with cortical cells, we measured the length of both types of epidermal cells in a subset of the same roots used above. The length of trichoblasts was similar to cortical cells throughout the apical part of the growth zone (Fig. 5A); the small difference in the first 75 μm from the quiescent center may reflect some (larger) root cap cells being mistakenly measured as epidermal cells. However, atrichoblasts were longer than the other cell types throughout the meristem (Fig. 5A).

Because trichoblasts had essentially the same cell length profiles as cortical cells, they also had similar cell division characteristics; however, atrichoblasts differed because they were larger than the other cell types at all positions. In atrichoblasts, cell flux increased more gradually and cell production rate was lower at all positions in the meristem (Fig. 5, B and C); however, despite the difference in cell production rate, the three cell types had rates of cell division that were not significantly different (Fig. 5D). Also, the cell types all ceased division at approximately the same distance from the quiescent center (Fig. 5D). Therefore, the lesser cell production in atrichoblast files resulted from there being fewer dividing cells per file, and this lessened cell number resulted from the larger size of atrichoblasts, not from slower divisions.

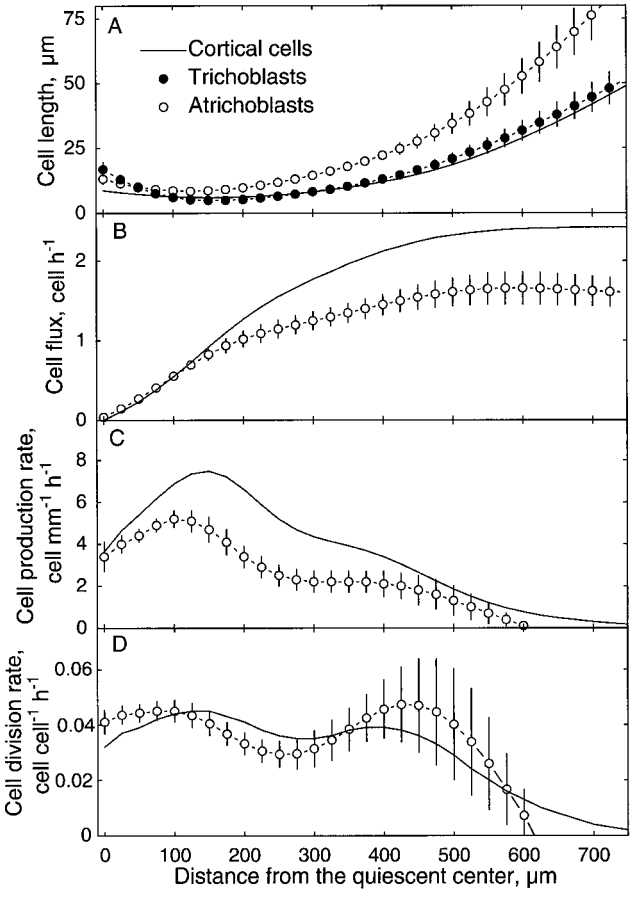

Figure 5. Spatial profiles of cell length and cell division parameters of epidermal cells. A, Cell length; because trichoblast cell length was similar to that of cortical cells, data for these cells are omitted from B to D for clarity. B, Cell flux; C, cell production rate; D, cell division rate. Data for cortical cells were re-drawn from Figures 3 and 4 and are shown for comparison. Data are for d 10. Symbols plot means ± SE (when larger than the symbol) for five roots.

DISCUSSION

The primary root of *A. thaliana* exhibited accelerated growth because the size of the growth zone increased. From d 6 to d 10, the root meristem produced cells more rapidly, but at all times the newly produced cells elongated in very nearly the same way. We hypothesize that the length of the zone of rapid elongation depends on the number of cells moving through it. In this view, each cell is endowed with a certain capacity for elongation; therefore, cell production rate, by determining the number of cells elongating at a given time, regulates root elongation rate directly.

Methodology

To measure the spatial profile of velocity, the time interval between successive observations was 1 h. This is a relatively long time for the determination of strain rates in roots; investigators often use an interval of 15 min. Our use of a longer period was necessary to determine accurately the low velocities in the meristem. The disadvantage of longer time intervals is a loss of accuracy, particularly at the basal end of the elongation zone, because of the considerable displacement of each particle. However, for this work the excess particle displacement was less than 20% of the length of the growth zone, which has been modeled to affect the calculated strain rate profiles negligibly (Peters and Bernstein, 1997).

The accelerating growth of *A. thaliana* roots presents a technical challenge. To our knowledge, the data presented here are the first published kinematic analyses of growth under non-steady-state conditions. At steady state, the term in Equation 4 expressing the local time-dependent change in cell density equals 0, and observations at a single time suffice for calculations (Sacks et al., 1997). We evaluated this term from observations made on the 3rd d and it was always less than 1 cell mm^{-1} h^{-1} and usually much less. Even though the magnitude of the time-dependent change in cell density was small, we included it in all of the results shown here; had it been omitted, the results would not have been changed materially.

The difference between smoothing methods (Fig. 1) illustrates the sensitivity of the calculations to sources of error. Therefore, we considered other possible sources of systematic error (measurement error is trivial compared with the variability in cell length or velocity). We found that potential misalignment of cell length and velocity data (due to errors in calibration factors or measurement of root cap length), the finite time that elapsed between the last velocity observation and cell length determination, and the movement of particles during the 1-h observation interval all had some effect on the calculated distributions of cell production and division rates. However, these effects were relatively small and did not materially affect our conclusions.

Division in Epidermal Cells

To our knowledge, differences in cell division parameters between trichoblasts and atrichoblasts have never been quantified before. We found that, whereas trichoblasts closely resembled cortical cells, atrichoblasts had lowered rates of cell production, extending up to the most apical part of the meristem; moreover, the lowered production rate was caused not by cells dividing more slowly but instead by their being longer and, consequently, fewer. The regulation of root hair formation in *A. thaliana* roots has been studied extensively, and many of the involved loci have been identified. When the expression of such loci has been studied, it has been found throughout the meristem, right up to the initials (Galway et al., 1994; Masucci et al., 1996). Our results show that the size divergence between the epidermal cell types originated in the very apical part of the meristem and was perpetuated by constant cell division rates; we suggest that epidermal cell fate is regulated in part through regulating the size of the initial cells.

Spatial Profile of Cell Division Rate

The spatial distribution of cell division rate has been estimated based on data from mitotic indices, tritiated-thymidine labeling, or colchicine blocking. Given the disruptive nature of these methods and their failure to account for the movement of cells during the labeling interval (Green and Bauer, 1977; Webster and Macleod, 1980), the results obtained, especially spatial aspects, must be interpreted with care. Our data indicate that cell division rates are approximately constant throughout the meristem (Fig. 4B). This agrees with kinematic observations in roots of maize (Barlow, 1987), onion (González-Fernández et al., 1968; Carmona and Cuadrado, 1986), and wheat (Hejnowicz, 1959) but is in contrast to other work on maize roots (Erickson and Sax, 1956; Sacks et al., 1997) and timothy grass (Goodwin and Avers, 1956; Hejnowicz, 1956; Erickson, 1961), which showed a bell-shaped distribution of cell division rate. Environmental differences may explain the different cell division patterns; however, another possibility is inadequate curve fitting. A bell-shaped curve may have resulted from oversmoothing, which tends to eliminate abrupt transitions; furthermore, most of the above study results had only a few data points in the meristem, which exacerbates the difficulty of curve fitting. Because we have many data points in the meristem and used a gentle smoothing approach applied to individual roots, the observed constancy of cell division rate is likely to be real. It remains to be determined to what extent the spatial profile of cell division rate can be affected by environmental conditions.

Proliferative Fraction

For years, scientists have debated the existence of a proliferative (or growth) fraction. It has been argued, on the basis of direct (Erickson, 1961; Bertaud and Gandar, 1985) and indirect (Balodis and Ivanov, 1970; Clowes, 1976) observations, that toward the base of the meristem an increasing proportion of cells leave the mitotic cycle, while only the proliferative fraction continues to divide. Because plant cells do not slide, a cell that stops dividing increases in length relative to cells that continue dividing by a factor of 2^n for each missed cycle. Consequently, if a proportion of cells left the cell cycle, the distribution of relative cell lengths found at the apical portion of the meristem would be narrower than at more basal positions. The main argument against the presence of cells that stop dividing much sooner than others is that the predicted differences in cell size between cells have been rarely observed (Webster and Macleod, 1980).

To determine whether any cells had stopped dividing early, we compared the distribution of cortical cell length in the apical part of the meristem (between 100 and 200 μm from the quiescent center) with that in the mature region of the root. In the apical part of the meristem, the proportion of cells lying outside the 2-fold size range expected if all cells divided exactly in half at the same length, was 17% (out of 673 cells from 5 roots), and in the mature region the proportion was 14% (out of 200 cells from 10 roots). That the proportion of cells exceeding the 2-fold range was low indicates a fairly close coordination of cell length and cell division. The similarity of the proportion between the distal meristem and the mature region shows that individual cells stopped dividing within one cell cycle of one another and, therefore, that cortical cells in *A. thaliana* roots continue to divide throughout the meristem (i.e. the proliferative fraction equals 1).

Actually, this observation is reconcilable with direct observations that some cells leave the cell cycle when they are near the center of the meristem. Given the fact that the cell cycle duration was approximately constant throughout the meristem, in one cell cycle the entire basal half of the meristem becomes displaced into the zone of rapid elongation (Ivanov, 1994). This means that cells originating from a division basal to the center of the meristem will have left the meristem before getting the chance to divide again. Direct observations of such cells following that division will show them to be nonproliferative, while adjacent cells will divide again.

Basal Terminus of the Meristem

Our results indicate that cell division in cortical and epidermal cell files continues well into the region where cell length increases rapidly (Fig. 3A) and where strain rates are severalfold higher than in the apical part of the meristem (Fig. 2B). This result agrees fully with data on the root meristems of timothy grass, wheat, and maize that were obtained by kinematic approaches (Goodwin and Stepka, 1945; Erickson and Sax, 1956; Goodwin and Avers, 1956; Hejnowicz, 1959; Sacks et al., 1997). However, this result conflicts with delineation of the meristem based on the distribution of mitoses seen in longitudinal sections, which typically find that the meristem ends at a more apical location, where cell lengths or strain rates are near their minimal values (Luxová, 1980; Barlow et al., 1991; Ishikawa and Evans, 1995).

We believe that, compared with mitotic indices, the kinematic determination of cell production delineates the basal terminus of the meristem more reliably. Scoring mitotic frequency in sections is difficult because as cell size increases, the frequency of nuclei decreases, and therefore the number of sections required to sample mitotic cells adequately at the basal end of the meristem becomes large. It is also possible that, as cell expansion accelerates, the duration of mitosis shortens, further reducing the frequency of mitotic cells. This would shorten the time a rapidly elongating cell spends without cortical microtubules, which are depolymerized during mitosis but are needed to control the directionality of cell expansion. Consistent with the terminus of the meristem defined kinematically, mitoses have been found in regions of considerable cell length or high strain rate (Jensen and Kavaljian, 1958; Rost and Baum, 1988). Therefore, for many species, the meristem very likely extends to regions where cells are relatively long and strain rates are high.

Physiologically, the basal portion of the meristem, where cell length and strain rate rapidly increase, is of great interest. An important role, distinct from other parts of the growth zone, is apparently played by this region in response to many different stimuli (Baluška et al., 1994; Ishikawa and Evans, 1995). This region was first called the "postmitotic isodiametric growth zone," since renamed "transition zone" (Baluška et al., 1996), and has been considered to be a region where cells recover from being mitotic and prepare for their phase of rapid expansion. However, according to our results as well as those in the literature (cited above), the basal part of the meristem extends into a region where cells expand rapidly. Interestingly, the transition zone approximately coincides with the location where cortical and epidermal cells are undergoing their final round of cell division; the final cell division may represent a specific developmental stage, during which cells possess distinctive characteristics. We concur with the recent proposal to name this region the transition zone but point out that the zone is a region where cells are undergoing their final division as well as expanding rapidly.

Cell Production and the Regulation of Organ Growth Rate

Cell production sustains growth; additionally, we suggest that cell production can regulate organ growth rate. The regulation of organ growth rate has traditionally been viewed from two distinct perspectives. The first is a purely spatial perspective, in which the position of the zone of rapid elongation and its size are considered to be specified by positional controls acting on the process of expansion. This view has been applied explicitly to morphogenesis (Cooke and Lu, 1992; Kaplan, 1992) and is commonly implicit in physiological studies that characterize spatial profiles of expansion (Sharp et al., 1988). The second perspective is cellular. Recognizing that the extent of the zone of rapid elongation is determined by the trajectory of the cells that move through it, the cellular view holds that the trajectory of the cells is specified when the cell is formed, just prior to its leaving the meristem. A model based on cells acting independently and even stochastically has been used to predict successfully a variety of organ level responses (Bradford and Trewavas, 1994). For root growth, a doubled cell production with no other change, in the spatial view, would halve the size of mature cells but would not change the size of the zone of rapid elongation or root elongation rate; in the cellular view, this would double the size of the zone of rapid elongation (and root elongation rate), because it would double the number of cells executing their set trajectories.

Spatial and cellular regulation are not incompatible and may both apply; nevertheless, we believe that cellular regulation is more important. The perspectives have not been distinguished by most studies of organ growth rate because they have found effects on both cell production and cellular elongation, so both processes were presumably affected independently. However, similar to the developmental example studied here in roots, there are several examples from studies of leaves in which an applied stress reduced the growth of the organ and the production of cells proportionally, without changing the elongation of individual cells (Terry et al., 1971; Lecoeur et al., 1995; Beemster et al., 1996). To explain these results on the leaf or the root, the spatial view must posit cell production and spatial control change in parallel, whereas the cellular view need posit a change in cell production only.

Further support for the cellular view comes from studies in which organ elongation is changed by treatments that should affect cell division specifically. First, cell division has been inhibited with γ rays, inhibitors of DNA synthesis, and by reducing the activity of the cell cycle regulator Cdc2 kinase, and organ elongation was considerably slowed (Foard and Haber, 1961; Barlow, 1969; Hemerly et al., 1995). However, these inhibitions of cell division were extreme and for that reason could have diminished elongation in response to some physiological disruption. More telling are treatments that stimulate cell production and increase organ elongation without affecting cellular elongation as judged by the approximately constant size of mature epidermal cells; this happened in roots of *A. thaliana* plants either mutant at the *AXR1* locus (Lincoln et al., 1990) or constitutively expressing a mitotic cyclin gene in the meristem (Doerner et al., 1996). The latter example is compelling because there is no obvious reason why the continuously expressed cyclin in the meristem should alter spatial controls on elongation. To explain these results, the spatial perspective must invoke linkages between cell division and the spatial control of elongation that are to date purely hypothetical, but the cellular perspective explains them easily by relating the changed organ growth directly to the changed flux of cells.

Finally, the hypothesis that the behavior of the zone of rapid elongation is controlled spatially predicts that cell production could be changed without changing the elongation of the organ. To our knowledge, no such example has been found. Note that the converse finding, changed elongation without changed cell production, fits either perspective because the changed elongation could result from changing either spatial controls or the endowment of each cell for elongation when it enters the zone of rapid elongation.

The number of examples in which division and expansion parameters have both been fully quantified is small, but such documentation must take place before the mechanisms that coordinate these processes can be productively explored. In this paper, we have shown for *A. thaliana* roots how a kinematic method allows division and expansion parameters of the whole growth zone to be measured accurately, and we have explained most of the developmental increase in elongation rate by increased cell production. It appears that cell number and temporally programmed cell behavior play important roles in regulating the growth of plant organs.

ACKNOWLEDGMENTS

We thank Jan Wilson for excellent technical assistance, Prof. Wendy Silk (University of California, Davis) for sharing results prior to publication, which gave us helpful insights for the analysis performed here, and Prof. Robert Sharp for his revelatory comments concerning the manuscript.

Received October 8, 1997; accepted January 11, 1998.
Copyright Clearance Center: 0032–0889/98/116/1515/12.

LITERATURE CITED

Balodis VA, Ivanov VB (1970) Proliferation of root cells in the basal part of meristem and apical part of elongation zone. Tsitologia **12:** 983–991 (in Russian)

Baluška F, Barlow PW, Kubica Š (1994) Importance of the postmitotic isodiametric growth (PIG) region for growth and development of roots. Plant Soil **167:** 31–41

Baluška F, Volkmann D, Barlow PW (1996) Specialized zones of development in roots. View from the cellular level. Plant Physiol **112:** 3–4

Barlow PW (1969) Cell growth in the absence of division in a root meristem. Planta **88:** 215–223

Barlow PW (1987) Cellular packets, cell division and morphogenesis in the primary root meristem of *Zea mays* L. New Phytol **105:** 27–56

Barlow PW, Brain P, Parker JS (1991) Cellular growth in roots of a gibberellin-deficient mutant of tomato (*Lycopersicon esculentum* Mill.) and its wild-type. J Exp Bot **42:** 339–351

Baskin TI, Cork A, Williamson RE, Gorst JR (1995) *STUNTED PLANT 1,* a gene required for expansion in rapidly elongating but not in dividing cells and mediating root growth responses to applied cytokinin. Plant Physiol **107:** 233–243

Baskin TI, Wilson JE (1997) Inhibitors of protein kinases and phosphatases alter root morphology and disorganize cortical microtubules. Plant Physiol **113:** 493–502

Beemster GTS, Masle J, Williamson RE, Farquhar GD (1996) Effects of soil resistance to root penetration on leaf expansion in wheat (*Triticum aestivum* L.): kinematic analysis of leaf elongation. J Exp Bot **47:** 1663–1678

Ben-Haj-Salah H, Tardieu F (1995) Temperature affects expansion rate of maize leaves without change in spatial distribution of cell length. Analysis of the coordination between cell division and cell expansion. Plant Physiol **109:** 861–870

Bertaud DS, Gandar PW (1985) Referential descriptions of cell proliferation in roots illustrated using *Phleum pratense* L. Bot Gaz **146:** 275–287

Bradford KJ, Trewavas AJ (1994) Sensitivity thresholds and variable time scales in plant hormone action. Plant Physiol **105:** 1029–1036

Carmona MJ, Cuadrado A (1986) Analysis of growth components in *Allium* roots. Planta **168:** 183–189

Clowes FAL (1976) Estimation of growth fractions in meristems of *Zea mays* L. Ann Bot **40:** 933–938

Cooke TJ, Lu B (1992) The independence of cell shape and overall form in multicellular algae and land plants: cells do not act as building blocks for constructing plant organs. Int J Plant Sci **153:** S7–S27

Doerner P, Jorgensen J, You R, Steppuhn J, Lamb C (1996) Control of root growth and development by cyclin expression. Nature **380:** 520–523

Dolan L (1996) Pattern in the root epidermis: an interplay of diffusible signals and cellular geometry. Ann Bot **77:** 547–553

Dolan L, Janmaat K, Willemsen V, Linstead P, Poethig S, Roberts K, Scheres B (1993) Cellular organisation of the *Arabidopsis thaliana* root. Development **119:** 71–84

Erickson RO (1961) Probability of division of cells in the epidermis of the *Phleum* root. Am J Bot **48:** 268–274

Erickson RO (1976) Modeling of plant growth. Annu Rev Plant Physiol **27:** 407–434

Erickson RO, Sax KB (1956) Rates of cell division and cell elongation in the growth of the primary root of *Zea mays*. Proc Am Philos Soc **100:** 499–514

Foard DE, Haber AH (1961) Anatomic studies of gamma radiated wheat growing without cell division. Am J Bot **48:** 438–446

Fujie M, Kuroiwa H, Kawano S, Kuroiwa T (1993) Studies on the behaviour of organelles and their nucleoids in the root apical meristem of *Arabidopsis thaliana* (L.) Col. Planta **189:** 443–452

Galway ME, Masucci JD, Lloyd AM, Walbot V, Davis RW, Schiefelbein JW (1994) The *TTG* gene is required to specify epidermal cell fate and cell patterning in the *Arabidopsis* root. Dev Biol **166:** 740–754

Gandar PW (1980) The analysis of growth and cell production in root apices. Bot Gaz **141:** 131–138

González-Fernández A, López-Sáez JF, Moreno P, Giménez-Martín G (1968) A model for dynamics of cell division cycle in onion roots. Protoplasma **65:** 263–276

Goodwin RH, Avers CJ (1956) Studies on roots. III. An analysis of root growth in *Phleum pratense* using photomicrographic records. Am J Bot **43:** 479–487

Goodwin RH, Stepka W (1945) Growth and differentiation in the root tip of *Phleum pratense*. Am J Bot **32:** 36–46

Green PB (1976) Growth and cell pattern formation on an axis: critique of concepts, terminology and modes of study. Bot Gaz **137:** 187–202

Green PB, Bauer K (1977) Analysing the changing cell cycle. J Theor Biol **68:** 299–315

Hejnowicz Z (1956) Growth and differentiation in the root of *Phleum pratense*. II. Distribution of cell divisions in the root. Acta Soc Bot Pol **25:** 615–628 (in Polish)

Hejnowicz Z (1959) Growth and cell division in the apical meristem of wheat roots. Physiol Plant **12:** 124–138

Hemerly AS, de Almeida Engler J, Bergounioux C, Van Montagu M, Engler G, Inzé D, Ferreira P (1995) Dominant negative mutants of the Cdc2 kinase uncouple cell division from iterative plant development. EMBO J **14:** 3925–3936

Ishikawa H, Evans ML (1995) Specialized zones of development in roots. Plant Physiol **109:** 725–727

Ivanov VB (1994) Root growth responses to chemicals. Sov Sci Rev D Physicochem Biol **13:** 1–70

Jensen WA, Kavaljian LG (1958) An analysis of cell morphology and the periodicity of division in the root tip of *Allium cepa*. Am J Bot **45:** 365–372

Kaplan DR (1992) The relationship of cells to organisms in intact plants: problem and implications of an organismal prerspective. Int J Plant Sci **153:** S28–S37

Lecoeur J, Wery J, Turc O, Tardieu F (1995) Expansion of pea leaves subjected to short water deficit: cell number and cell size are sensitive to stress at different periods of leaf development. J Exp Bot **46:** 1093–1101

Lincoln C, Britton JH, Estelle M (1990) Growth and development of the *axr1* mutants of Arabidopsis. Plant Cell **2:** 1071–1080

Luxová M (1980) Kinetics of miaze root growth. Ukr Bot Zh **37:** 68–72 (in Ukrainian)

Masucci JD, Rerie WG, Foreman DR, Zhang M, Galway ME, Marks MD Schiefelbein JW (1996) The homeobox gene *GLABRA 2* is required for position dependent cell differentiation in

the root epidermis of *Arabidopsis thaliana*. Development **122:** 1253–1260

Morris AK, Silk WK (1992) Use of a flexible logistic function to describe axial growth of plants. Bull Math Biol **54:** 1069–1081

Peters WS, Bernstein N (1997) The determination of relative elemental growth rate profiles from segmental growth rates—a methodological evaluation. Plant Physiol **113:** 1395–1404

Rost TL, Baum S (1988) On the correlation of primary root length, meristem size and protoxylem tracheary element position in pea seedlings. Am J Bot **75:** 414–424

Sacks MM, Silk WK, Burman P (1997) Effect of water stress on cortical cell division rates within the apical meristem of primary roots of maize. Plant Physiol **114:** 519–527

Sharp RE, Silk WK, Hsiao TC (1988) Growth of the maize primary root at low water potentials. I. Spatial distribution of expansive growth. Plant Physiol **87:** 50–57

Silk WK (1984) Quantitative descriptions of development. Annu Rev Plant Physiol **35:** 479–518

Silk WK, Erickson RO (1979) Kinematics of plant growth. J Theor Biol **76:** 481–501

Terry N, Waldron LJ, Ulrich A (1971) Effects of moisture stress on the multiplication and expansion of cells in leaves of sugar beet. Planta **97:** 281–289

Webster PL, Macleod RD (1980) Characteristics of root apical meristem cell population kinetics: a review of analyses and concepts. Environ Exp Bot **20:** 335–358